

# THEORETICAL AND CONDENSED MATTER PHYSICS

October 19-21, 2017 New York, USA

## Universal and system-specific charge density wave features in 2H-transition metal dichalcogenides

Utpal Chatterjee  
University of Virginia, USA

Recently, the studies of incommensurate charge density wave (CDW) phases in various 2H-polytypes of transition metal dichalcogenides (TMDs), e.g., 2H-NbSe<sub>2</sub> and 2H-TaSe<sub>2</sub>, have attracted a lot of attention due to intriguing experimental observations, some of which are reminiscent of the enigmatic pseudogap phase in cuprate high temperature superconductors (HTSCs). We present a comprehensive Angle Resolved Photoemission spectroscopy (ARPES) study on 2H-TaS<sub>2</sub>, a canonical incommensurate CDW material. Comparing our ARPES data together with arguments based on a tight-binding analysis on 2H-TaS<sub>2</sub>, with those on related materials like 2H-NbSe<sub>2</sub> and 2H-TaSe<sub>2</sub>, we identify the generic and system-specific characteristics of these systems. We find the following generic features of incommensurate CDW TMDs: (i) opening of CDW energy gap ( $\Delta_{cdw}$ ) along part of the underlying Fermi Surface (FS) sheets; (ii) finite  $\Delta_{cdw}$  at temperatures above the CDW transition temperatures and particle-hole asymmetry in  $\Delta_{cdw}$  and a lack of one-to-one correspondence between CDW wave vectors and the FS nesting vectors. We have also observed some system-specific features. For example, in contrast to 2H-NbSe<sub>2</sub>, where  $\Delta_{cdw}$  is non-zero only at a few “hot spots” on a specific FS sheet,  $\Delta_{cdw}$  in 2H-TaS<sub>2</sub> is non-zero along the entirety of multiple FS sheets. Using a tight-binding model, we describe this in terms of the difference in the orbital orientations of their electronic states close to the Fermi level. In short, our strong-coupling model can describe both the generic and the material-specific features of these compounds. Therefore, we argue that the strong electron-phonon coupling, including its orbital and momentum-dependence, is key to the incommensurate CDW instability in TMDs.

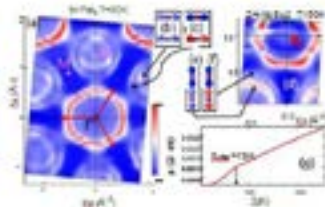


FIG. 1. (a) ARPES intensity map of a 2H-TaS<sub>2</sub> sample obtained using a 400 eV photon source at an energy resolution of 10 meV. The red arrows correspond to the Fermi surface sheets. The blue arrows correspond to the CDW wave vectors. (b) The intensity map along the Brillouin zone showing the CDW gap opening. The red line indicates the CDW wave vector. (c) The Fermi surface map of a 2H-TaS<sub>2</sub> sample at T = 50 K using a 400 eV photon source. The red arrows indicate the Fermi surface sheets. (d) The Fermi surface map of a 2H-TaS<sub>2</sub> sample at T = 50 K using a 400 eV photon source. The red arrows indicate the Fermi surface sheets. (e) The Fermi surface map of a 2H-TaS<sub>2</sub> sample at T = 50 K using a 400 eV photon source. The red arrows indicate the Fermi surface sheets. (f) The Fermi surface map of a 2H-TaS<sub>2</sub> sample at T = 50 K using a 400 eV photon source. The red arrows indicate the Fermi surface sheets. (g) The Fermi surface map of a 2H-TaS<sub>2</sub> sample at T = 50 K using a 400 eV photon source. The red arrows indicate the Fermi surface sheets. (h) The Fermi surface map of a 2H-TaS<sub>2</sub> sample at T = 50 K using a 400 eV photon source. The red arrows indicate the Fermi surface sheets. (i) The Fermi surface map of a 2H-TaS<sub>2</sub> sample at T = 50 K using a 400 eV photon source. The red arrows indicate the Fermi surface sheets. (j) The Fermi surface map of a 2H-TaS<sub>2</sub> sample at T = 50 K using a 400 eV photon source. The red arrows indicate the Fermi surface sheets. (k) The Fermi surface map of a 2H-TaS<sub>2</sub> sample at T = 50 K using a 400 eV photon source. The red arrows indicate the Fermi surface sheets. (l) The Fermi surface map of a 2H-TaS<sub>2</sub> sample at T = 50 K using a 400 eV photon source. The red arrows indicate the Fermi surface sheets. (m) The Fermi surface map of a 2H-TaS<sub>2</sub> sample at T = 50 K using a 400 eV photon source. The red arrows indicate the Fermi surface sheets. (n) The Fermi surface map of a 2H-TaS<sub>2</sub> sample at T = 50 K using a 400 eV photon source. The red arrows indicate the Fermi surface sheets. (o) The Fermi surface map of a 2H-TaS<sub>2</sub> sample at T = 50 K using a 400 eV photon source. The red arrows indicate the Fermi surface sheets. (p) The Fermi surface map of a 2H-TaS<sub>2</sub> sample at T = 50 K using a 400 eV photon source. The red arrows indicate the Fermi surface sheets. (q) The Fermi surface map of a 2H-TaS<sub>2</sub> sample at T = 50 K using a 400 eV photon source. The red arrows indicate the Fermi surface sheets. (r) The Fermi surface map of a 2H-TaS<sub>2</sub> sample at T = 50 K using a 400 eV photon source. The red arrows indicate the Fermi surface sheets. (s) The Fermi surface map of a 2H-TaS<sub>2</sub> sample at T = 50 K using a 400 eV photon source. The red arrows indicate the Fermi surface sheets. (t) The Fermi surface map of a 2H-TaS<sub>2</sub> sample at T = 50 K using a 400 eV photon source. The red arrows indicate the Fermi surface sheets. (u) The Fermi surface map of a 2H-TaS<sub>2</sub> sample at T = 50 K using a 400 eV photon source. The red arrows indicate the Fermi surface sheets. (v) The Fermi surface map of a 2H-TaS<sub>2</sub> sample at T = 50 K using a 400 eV photon source. The red arrows indicate the Fermi surface sheets. (w) The Fermi surface map of a 2H-TaS<sub>2</sub> sample at T = 50 K using a 400 eV photon source. The red arrows indicate the Fermi surface sheets. (x) The Fermi surface map of a 2H-TaS<sub>2</sub> sample at T = 50 K using a 400 eV photon source. The red arrows indicate the Fermi surface sheets. (y) The Fermi surface map of a 2H-TaS<sub>2</sub> sample at T = 50 K using a 400 eV photon source. The red arrows indicate the Fermi surface sheets. (z) The Fermi surface map of a 2H-TaS<sub>2</sub> sample at T = 50 K using a 400 eV photon source. The red arrows indicate the Fermi surface sheets.

### Biography

Utpal Chatterjee has completed his PhD from University of Illinois at Chicago in 2007. Afterwards, he has conducted his Postdoctoral studies at Materials Science Division of Argonne National Laboratory with Director’s fellowship. He has joined University of Virginia in 2012. His research is focused on experimental study of strongly correlated electronic systems. His principal expertise is in angle resolved photoemission spectroscopy. His research over past 10 years has produced many high impact publications, which include Nat. Commun, 2015; 6: 6313 DOI: 10.1038/ncomms 7313, Nat. Phys. 10, 357; PNAS 110, 17774; PNAS 108, 9346; Nat. Phys. 6, 99; PRL 96, 107006.

uc5j@eservices.virginia.edu

### Notes: